applied sciences

MDPI

Article

Fast Sparse Bayesian Learning-Based Channel Estimation for Underwater Acoustic OFDM Systems

Yong-Ho Cho

Department of Information and Communication Engineering, Mokpo National University, Muan 58554, Korea; yonghocho@mnu.ac.kr

Abstract: Harsh underwater channels and energy constraints are the two critical issues of underwater acoustic (UWA) communications. To achieve a high channel estimation performance under a severe underwater channel, sparse Bayesian learning (SBL)-based channel estimation was adopted for UWA orthogonal frequency division multiplexing (OFDM) systems. Accurate channel estimation can guarantee the successful reception of transmitted data and reduce retransmission occurrences, thereby, leading to energy-efficient communications. However, SBL-based algorithms have improved performances in iterative ways, which require high power consumption. In this paper, a fast SBL algorithm based on a weighted learning rule for hyperparameters is proposed for channel estimation in a UWA-OFDM system. It was shown via numerical analysis that the proposed weighted learning rule enables fast convergence and more accurate channel estimation simultaneously. Simulation results confirm that the proposed algorithm achieves higher accuracy in channel estimation with much fewer iteration numbers in comparison to conventional SBL-based methods for a time-varying UWA channel.

Keywords: orthogonal frequency division multiplexing (OFDM); sparse Bayesian learning (SBL); underwater acoustic communications; channel estimation

Citation: Cho, Y.-H. Fast Sparse Bayesian Learning-Based Channel Estimation for Underwater Acoustic OFDM Systems. *Appl. Sci.* **2022**, *12*, 10175. https://doi.org/10.3390/app121910175

Academic Editor: Jie Tian

Received: 8 September 2022
Accepted: 29 September 2022
Published: 10 October 2022

Publisher's Note: MDPI stays neutral with regard to jurisdictional claims in published maps and institutional affiliations.

1. Introduction

Utilization of an underwater sensor network (USN) or autonomous underwater vehicles (AUVs), or both, for military, science, and industrial applications is receiving increasing attention [1,2]. In order to advance underwater applications, underwater acoustic (UWA) communication is essential for establishing connectivity between devices, sensors, and AUVs.

Energy constraints are critical in UWA communications. In the case of USN, replacing or charging the batteries of sensor nodes leads to huge costs and might not be practical in some networks. The lifetime of the battery heavily determines the range and duration of AUV operation. For energy-efficient communication, a UWA-OFDM receiver with low-power consumption is indispensable. To achieve energy-efficient communication, retransmission occurrences should also be minimized so that unnecessary power consumption via retransmission can be prevented.

Recently, orthogonal frequency division multiplexing (OFDM) has been studied for UWA communication systems due to the advantages (e.g., high robustness to multi-paths). The UWA channel is known to be very difficult in communication media because it suffers from fast time-varying characteristics in time and frequency domains, resulting in multi-paths with long delays as well as a severe Doppler effect [3]. Under a harsh UWA channel, accurate channel estimation is crucial to fully enjoy the advantages of an OFDM-based modulation technique. Accurate channel estimation also leads to the successful reception of data and reduction of retransmission occurrences, thereby, achieving energy-efficient communication.

For UWA-OFDM systems, channel estimators (CEs) based on the principle of compressed sensing (CS) [4–6] and sparse Bayesian learning (SBL) [7] have been proposed, both of which operate in iterative ways to achieve high channel estimation performances. For further accuracy, many variants based on the principle of SBL [8–10] including temporal multiple SBL (TMSBL) [7,11], and partition-based clustered-sparse Bayesian learning (PB-CSBL) [12] have recently been proposed. Improved performances of SBL-based algorithms lead to successful decoding of transmitted data, resulting in no retransmission. However, this performance gain is obtained through iterative operations, which consume much more battery power compared to non-iterative methods.

In this paper, a fast SBL (F-SBL) algorithm is proposed for channel estimation in the UWA-OFDM system. The proposed method uses the weighted learning rule (LR) for hyperparameters. It has been shown by numerical analysis that weighted LR enables the SBL estimator (to converge faster and achieve a more accurate channel estimation). Simulation results confirm that the proposed technique shows an improved performance compared to conventional SBL-based methods [5,7,13], with fewer iteration numbers.

2. System Model

We considered a UWA OFDM with N subcarriers, where the N_U subcarriers carry data and pilot symbols, and the remaining $N_G/2$ subcarriers at each edge of the spectrum are used for guard bands. In the time and frequency domain, the pilot symbols are allocated in a comb-type fashion with the spacing of D_f subcarriers and D_t OFDM symbols. Let I_f and $N_f = |I_f|$ denote the subcarrier indices and the number of pilot symbols in the frequency domain, respectively. Similarly, let I_t and $N_t = |I_t|$ denote the OFDM symbol indices and the number of pilot symbols in the time domain, respectively.

The time domain sample of the i-th OFDM symbol $s_i[n]$ is represented as

$$s_i[n] = \frac{1}{\sqrt{N}} \sum_{k=0}^{N-1} S_i(k) e^{j\frac{2\pi}{N}kn}, \; n = 0, \cdots, N-1. \tag{1}$$

where $S_i(k)$ is the symbol on the k-th subcarrier of the i-th OFDM symbol. In order to maintain orthogonality between subcarriers under a frequency selective channel, a CP (of N_{cp} samples) is appended to the beginning of each OFDM symbol. After the CP insertion, the time domain samples are then pulse-shaped and up-converted to the carrier frequency f_c. In the passband, the resulting transmitted signal is given by

$$\tilde{s}(t) = 2\mathrm{Re}\left(\sum_{i=0}^{N_{sym}-1} \sum_{n=-N_{cp}}^{N-1} s_i[n] u(t - (iN_s + n)t_s) \right) e^{j2\pi f_c t} \tag{2}$$

where $u(t)$ is a pulse-shaped filter, $N_s = N + N_{cp}$, and N_{sym} and t_s denote the number of transmitted OFDM symbols and the sample duration, respectively.

The time-varying UWA channel is often modeled as [5,14,15]

$$h(\tau, t) = \sum_{l=0}^{N_{path}-1} c_l(t)\, \delta(\tau - \tau_l(t)) \tag{3}$$

where N_{path} is the number of channel taps, and $c_l(t)$ and $\tau_l(t)$ denote the time-varying path gain and delay of the l-th channel tap, respectively. It can be assumed that during an OFDM symbol, the path gain of each tap is time-invariant, while its delay is time-varying by the Doppler effect [5]:

$$\begin{aligned} c_l(t) &= c_l, \\ \tau_l(t) &= \tau_l - \alpha_l t, \end{aligned} \tag{4}$$

where α_l is the Doppler rate of the l-th channel tap. The channel impulse response (CIR) can then be rewritten as

$$h(\tau, t) = \sum_{l=0}^{N_{path}-1} c_l \, \delta(\tau - \tau_l + \alpha_l t). \tag{5}$$

The passband representation of the received signal is given as

$$y(t) = \sum_{l=0}^{N_{path}-1} c_l \, \tilde{s}(t - \tau_l + \alpha_l t) + w(t) \tag{6}$$

where $w(t)$ is the additive white Gaussian noise (AWGN) with a zero mean and variance σ_n^2.

At the receiver, it is assumed that a two-step approach is applied to the received signal in (6) to mitigate the Doppler effect, which performs resampling in the passband and subsequently compensates the Doppler shift [5,16]. For ease of derivation, we assume no residual Doppler rate, i.e., $\alpha_l = 0, \ \forall l$ with the aid of resampling and Doppler shift compensation. Then, the CIR in (5) can be rewritten to a time-invariant tapped–delay–line model as follows:

$$h(\tau) = \sum_{l=0}^{N_{path}-1} c_l \, \delta(\tau - \tau_l) \tag{7}$$

After resampling, the received pilot symbols carried by the i-th OFDM symbol in the baseband is represented as

$$\mathbf{y}_i = \mathbf{X}_i \mathbf{A} \mathbf{h} + \mathbf{A} \mathbf{w}, \ i \in I_t \tag{8}$$

where $\mathbf{X}_i$ is an $N_f \times N_f$ diagonal matrix composed of the pilot symbols in the i-th OFDM symbol, $\mathbf{A}$ is an $N_f \times N_{path}$ DFT matrix with entries $[\mathbf{A}]_{m,n} = \frac{1}{\sqrt{N}} e^{-j\frac{2\pi}{N} I_f(m) n}$, $\mathbf{h} = [h(0), \ h(1), \cdots, \ h(N_{path} - 1)]^T$ is a time-invariant $N_{path} \times 1$ CIR vector, and $\mathbf{w}$ is an AWGN vector.

3. Proposed CE Method

3.1. SBL-Based CE

In the SBL-based CE framework, we assume the Gaussian likelihood model as

$$p(\mathbf{y}_i | \mathbf{h}) = \frac{1}{(\pi \sigma_n^2)^{N_{path}}} e^{-\frac{||\mathbf{y}_i - \mathbf{\Phi}_i \mathbf{h}||^2}{\sigma_n^2}} \tag{9}$$

where $\mathbf{\Phi}_i = \mathbf{X}_i \mathbf{A}$. The objective is to estimate each tap of the CIR, and it is assumed that each tap of the CIR follows independently and is identically distributed (i.i.d.) with a complex Gaussian distribution as

$$h(l) \sim \mathcal{CN}(0, \gamma_l), \tag{10}$$

where γ_l is the prior variance corresponding to the l-th tap of the CIR, which is treated as a deterministic but unknown hyperparameter. The parameterized Gaussian prior is given by

$$p(\mathbf{h}; \mathbf{\Gamma}) = \prod_{l=0}^{N_{path}-1} \frac{1}{\pi \gamma_l} e^{-\frac{|h_l|^2}{\gamma_l}} \tag{11}$$

where $\mathbf{\Gamma} = \mathrm{diag}\Big(\gamma_0, \ \gamma_1 \ \cdots, \ \gamma_{N_{path}-1}\Big)$ is the diagonal matrix of hyperparameters. The hyperparameters can be estimated by performing ML optimization of the marginalized probability density function (pdf) $p(\mathbf{y}_i; \mathbf{\Gamma})$ [17]:

$$\tilde{\mathbf{\Gamma}} = \arg\max_{\mathbf{\Gamma}} p(\mathbf{y}_i; \mathbf{\Gamma}). \tag{12}$$

where the marginalized pdf is given by

$$\begin{aligned} p(\mathbf{y}_i;\mathbf{\Gamma}) &= \int p(\mathbf{y}_i|\mathbf{h})p(\mathbf{h};\mathbf{\Gamma})d\mathbf{h} \\ &= \pi^{-N_{path}}|\Sigma_y|^{-1}e^{-\mathbf{y}_i^H\Sigma_y^{-1}\mathbf{y}_i}. \end{aligned} \tag{13}$$

The ML optimization in (12), which is called type-II ML, cannot be solved in closed form. Accordingly, in the SBL-based CE framework, the expectation maximization (EM) algorithm is employed to maximize $p(\mathbf{y}_i;\mathbf{\Gamma})$ [17–19]. Note that the EM algorithm guarantees convergence to local optima and low complexity [20]. The EM algorithm treats the CIR vectors $\mathbf{h}$ as hidden variables and estimates $\mathbf{\Gamma}$ in an iterative way. The E and M steps of the EM algorithm for the k-th step is given as

$$\begin{aligned} E\ step: &\mathcal{L}\left(\mathbf{\Gamma}|\mathbf{\Gamma}^{(k-1)}\right) = \mathbb{E}_{\mathbf{h}|\mathbf{y}_i;\mathbf{\Gamma}^{(k-1)}}[\log p(\mathbf{y}_i,\mathbf{h};\mathbf{\Gamma})] \\ M\ step: &\mathbf{\Gamma}^{(k)} = \arg\max_{\mathbf{\Gamma}} \mathcal{L}\left(\mathbf{\Gamma}|\mathbf{\Gamma}^{(k-1)}\right) \end{aligned} \tag{14}$$

In order to solve the maximization in the M-step, we rewrite the E-step as

$$\begin{aligned} \mathcal{L}\left(\mathbf{\Gamma}|\mathbf{\Gamma}^{(k-1)}\right) &= \mathbb{E}_{\mathbf{h}|\mathbf{y}_i;\mathbf{\Gamma}^{(k-1)}}[\log p(\mathbf{y}_i,\mathbf{h};\mathbf{\Gamma})] \\ &= \mathbb{E}_{\mathbf{h}|\mathbf{y}_i;\mathbf{\Gamma}^{(k-1)}}[\log p(\mathbf{y}_i|\mathbf{h};\mathbf{\Gamma}) + \log p(\mathbf{h};\mathbf{\Gamma})] \\ &= \mathbb{E}_{\mathbf{h}|\mathbf{y}_i;\mathbf{\Gamma}^{(k-1)}}[\log p(\mathbf{h};\mathbf{\Gamma})] \end{aligned} \tag{15}$$

Note that the term $\mathbb{E}_{\mathbf{h}|\mathbf{y}_i;\mathbf{\Gamma}^{(k-1)}}[\log p(\mathbf{y}_i|\mathbf{h};\mathbf{\Gamma})]$ is removed in the last equality in (15) because $p(\mathbf{y}_i|\mathbf{h};\mathbf{\Gamma})$ in (9) does not depend on the hyperparameter matrix $\mathbf{\Gamma}$. Then, the M-step can be rewritten as

$$\begin{aligned} \mathbf{\Gamma}^{(k)} &= \arg\max_{\mathbf{\Gamma}} \mathcal{L}\left(\mathbf{\Gamma}|\mathbf{\Gamma}^{(k-1)}\right) \\ &= \arg\max_{\mathbf{\Gamma}} \mathbb{E}_{\mathbf{h}|\mathbf{y}_i;\mathbf{\Gamma}^{(k-1)}}[\log p(\mathbf{h};\mathbf{\Gamma})] \\ &= -\arg\max_{\mathbf{\Gamma}} \sum_{l=0}^{N_{path}-1}\left[\log(\pi\gamma_l) + \frac{1}{\gamma_l}\mathbb{E}_{\mathbf{h}|\mathbf{y}_i;\mathbf{\Gamma}^{(k-1)}}\left[|h_l|^2\right]\right] \end{aligned} \tag{16}$$

The maximization in (16) can be decoupled with respect to each γ_l. Differentiating the objective function with each γ_l and letting the derivative equal to zero yields the estimate $\gamma_l^{(k)}$ as

$$\gamma_l^{(k)} = \mathbb{E}_{\mathbf{h}|\mathbf{y}_i;\mathbf{\Gamma}^{(k-1)}}\left[|h_l|^2\right] \tag{17}$$

The above requires *a posteriori* the pdf of the CIR vector $\mathbf{h}$, which is written as

$$p(\mathbf{h}|\mathbf{y}_i;\mathbf{\Gamma}^{(k-1)}) = \mathcal{CN}\left(\mu^{(k)},\mathbf{\Sigma}^{(k)}\right) \tag{18}$$

where

$$\begin{aligned} \mu^{(k)} &= \frac{1}{\sigma_n^2}\mathbf{\Sigma}^{(k)}\mathbf{\Phi}_i^H\mathbf{y}_i \\ \mathbf{\Sigma}^{(k)} &= \left(\frac{1}{\sigma_n^2}\mathbf{\Phi}_i^H\mathbf{\Phi}_i + \left(\mathbf{\Gamma}^{(k-1)}\right)^{-1}\right)^{-1}. \end{aligned} \tag{19}$$

Then, the M step in (17) can be simplified to

$$\gamma_l^{(k)} = [\mathbf{\Sigma}^{(k)}]_{l,l} + |[\mu^{(k)}]_l|^2 \tag{20}$$

Regarding convergence, a maximum a posteriori estimate of $\mathbf{h}$ is given as $\tilde{\mathbf{h}} = \mu$.

3.2. Fast SBL-Based CE

In the EM algorithm, at the E step, the posterior covariance matrix $\mathbf{\Sigma}$ is computed with $\mathbf{\Gamma}$, and the posterior mean μ is computed with the $\mathbf{\Sigma}$. Then, $\mathbf{\Gamma}$ is updated based on $\mathbf{\Sigma}$ and μ at the M step. These updates are performed alternatively at every iteration until convergence. Upon convergence, many of the diagonal components of $\mathbf{\Gamma}$, γ_l converge to zero and so do the corresponding $[\mu]_l$, resulting in sparse estimates of the CIR vector $\mathbf{h}$ [17]. To investigate the convergence behavior of the SBL-based CE, μ, diagonal elements of $\mathbf{\Sigma}$, and $\mathbf{\Gamma}$ at the first, second, and fifth iterations are represented in Figure 1b–d, respectively, for a given time-invariant CIR depicted in Figure 1a. It can be observed that the diagonal elements of $\mathbf{\Sigma}$ decrease while $\mathbf{\Gamma}$ converges to μ as the iteration progresses. It is also noted that μ and $\mathbf{\Gamma}$ become more sparse, in which distinct components become more dominant while insignificant components diminish substantially.

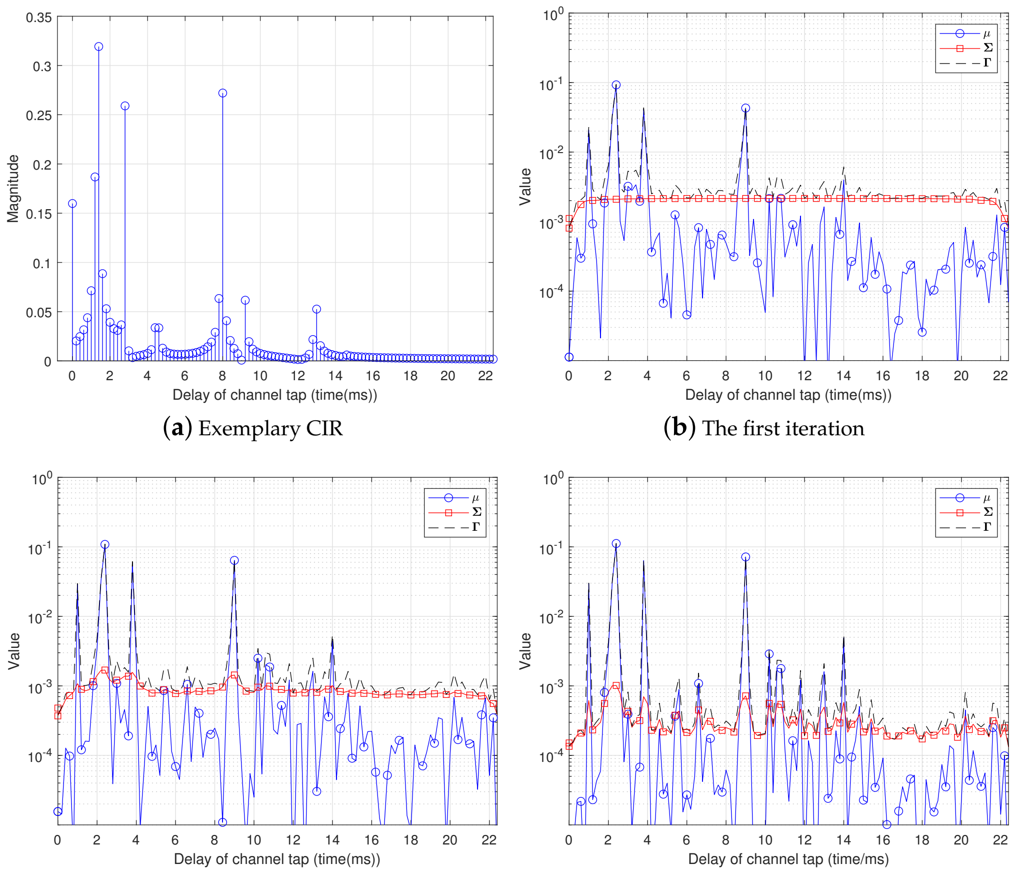

(**a**) Exemplary CIR (**b**) The first iteration

(**c**) The second iteration (**d**) The fifth iteration

Figure 1. Exemplary CIR and μ, $\mathbf{\Sigma}$, and $\mathbf{\Gamma}$ at the first, second, and fifth iterations.

For faster convergence, the observations from Figure 1 suggest the following conditions:

Condition 1: diagonal elements of $\mathbf{\Sigma}$ need to have small values.

Condition 2: $\mathbf{\Gamma}$ should be determined more by μ rather than the diagonal elements of $\mathbf{\Sigma}$.

To achieve the above conditions, we propose a new LR for $\mathbf{\Gamma}$ as

$$\gamma_l^{(k)} = w_1 \left[\mathbf{\Sigma}^{(k)}\right]_{l,l} + w_2 \left| \left[\mu^{(k)}\right]_l \right|^2 \tag{21}$$

where w_1 and w_2 control the weights of the diagonal elements of $\mathbf{\Sigma}$ and μ in the update of $\mathbf{\Gamma}$.

The judicious selection of weights w_1 and w_2 can achieve the above conditions rapidly, accelerating the convergence, which will be discussed in the following subsection. The proposed F-SBL algorithm is summarized in Algorithm 1.

Algorithm 1 F-SBL algorithm.

Input: $\mathbf{y}_i$ and $\mathbf{\Phi}_i$ for $\forall i \in I_t$, stopping parameter ϵ_0, the maximum number of iterations N_{iter}, weights w_1 and w_2, noise variance σ_n^2
Output: $\tilde{\mathbf{h}}_i$ for $\forall i \in I_t$
1: **for** $i = 0$ to $|I_t| - 1$ **do**
2: Initialization: $\mathbf{\Gamma}^{(0)} = \frac{1}{N_{path}} \mathbf{I}_{N_{path}}$ and $k = 0$
3: **while** $||\mathbf{\Gamma}^{(k)} - \mathbf{\Gamma}^{(k-1)}||_F^2 > \epsilon_0$ and $k < N_{iter}$ **do**
4: $k \leftarrow k + 1$
5: $\mathbf{\Sigma}^{(k)} \leftarrow \left(\frac{1}{\sigma_n^2} \mathbf{\Phi}_i^H \mathbf{\Phi}_i + \left(\mathbf{\Gamma}^{(k-1)} \right)^{-1} \right)^{-1}$
6: $\mu^{(k)} \leftarrow \frac{1}{\sigma_n^2} \mathbf{\Sigma}^{(k)} \mathbf{\Phi}_i \mathbf{y}_i$
7: $\gamma_l^{(k)} \leftarrow w_1 \left[\mathbf{\Sigma}^{(k)} \right]_{l,l} + w_2 \left| \left[\mu^{(k)} \right]_l \right|^2, l = 0, \cdots, N_{path} - 1$
8: **end while**
9: $\tilde{\mathbf{h}}_i \leftarrow \mu^{(k)}$
10: **end for**

3.3. Performance Analysis

Firstly, we examined the performance of the proposed F-SBL algorithm according to weights w_1 and w_2. Since the proposed update formula for $\mathbf{\Gamma}$ in (21) is apart from the derivation based on *a posteriori* pdf $p(\mathbf{h}|\mathbf{y}_i; \mathbf{\Gamma}^{(k-1)})$ in (20), it was difficult to investigate the effect of the weights analytically, and, according, we adopted a numerical approach.

As a performance metric, the mean squared error for the channel frequency response was used:

$$\text{MSE} = \frac{1}{N_U} tr\Big(E\big[(\tilde{\mathbf{H}} - \mathbf{H})(\tilde{\mathbf{H}} - \mathbf{H})^H \big] \Big), \tag{22}$$

where $\mathbf{H} = \mathbf{Q}\mathbf{h}$, $\tilde{\mathbf{H}} = \mathbf{Q}\tilde{\mathbf{h}}$, and $\mathbf{Q}$ is a $N_U \times N_{path}$ DFT matrix with entries $[\mathbf{Q}]_{m,n} = e^{-j\frac{2\pi}{N}(m+N_G/2)n}$. Note that the CIR vector in the MSE is time-invariant. For the MSE analysis, a sparse channel having $N_{path} = 8$ taps is used. In particular, the delay of each path is randomly distributed within 15 ms, where the minimum difference between adjacent paths is set to 1 ms. The path gain decreases exponentially, where the difference between the first and the last paths is 25 dB. The Doppler rate for each path α_l is set to 0 so that the resultant channel is time-invariant. The UWA OFDM system with parameters summarized in Table 1 is used for the following analysis.

Table 1. Parameters of the UWA OFDM system.

Carrier Frequency	f_c	12 kHz
Bandwidth	B	5 kHz
Sampling frequency	f_s	5 kHz
No. of total subcarriers	N	512
No. of useful subcarriers	N_U	400
No. of null subcarriers	N_G	109
pilot symbols spacing in freq.	D_f	4
pilot symbols spacing in time	D_t	2
No. of preambles	$N_{preamble}$	2
No. of OFDM symbols	N_{sym}	16
OFDM block duration	T_b	125 ms
CP duration	T_{CP}	22.6 ms

The MSE performance of the proposed method according to different values of weights w_1 and w_2 is shown for SNR = 12 dB in Figure 2, where the number of iterations N_{iter} is set to 5. It can be observed from the figure that weights smaller than 1.0 improved the performance compared with the case of $w_1 = w_2 = 1$, which is equivalent to the conventional SBL method in (20). The optimal weights are yielded as $w_1^* = 0.4$ and $w_2^* = 0.6$. Note that the optimal weights agreed with conditions 1 and 2 derived in the previous subsection. Specifically, both optimal weights smaller than 1.0 supported condition 1, while $w_1^* < w_2^*$ justified condition 2.

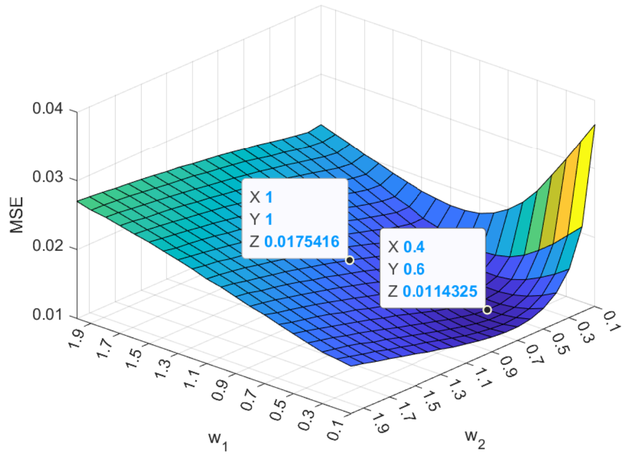

Figure 2. The MSE performance of the proposed F-SBL algorithm according to different values of weights w_1 and w_2 for SNR = 12 dB.

We now investigate the convergence rate of the proposed F-SBL algorithm. Figure 3 shows the MSE performance of the proposed method with various weights and the conventional SBL method ($w_1 = 1.0$ and $w_2 = 1.0$) according to the iteration index for SNR = 10 dB. The same channel for the results in Figure 2 was used. Firstly, it can be clearly seen that the proposed F-SBL algorithms with weights smaller than 1 converged more rapidly than the conventional SBL method. We observed that the proposed method with weights smaller than the optimal ($w_1 = 0.2$ and $w_2 = 0.3$) reached the minimum at the iteration index $k = 3$, showing faster convergence than the one with the optimal weights, but its MSE performance degraded as the iteration progressed. On the other hand, the proposed method with weights larger than the optimal ($w_1 = 0.6$ and $w_2 = 0.8$) exhibited slower convergence performance. In the case that the weights were larger than 1, the performance was severely degraded, showing poor MSE compared to the conventional SBL method. The proposed method with the optimal weights yielded the least MSE over the one with the non-optimal weights at iteration index $k = 6$. Therefore, it was expected from the results that the proposed method with the optimal weights would provide a more accurate channel estimation with fewer iterations compared with the conventional SBL method. It is worth noting that the proposed LR in (21) can be applied easily to other SBL-based algorithms [7,11,12] and can improve the convergence rate and estimation performance simultaneously.

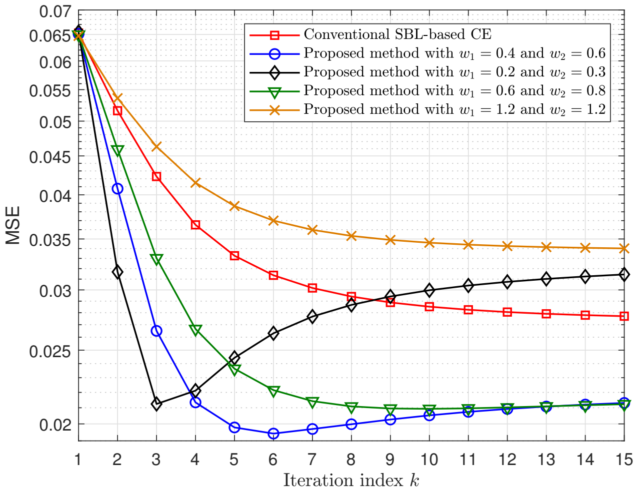

Figure 3. The convergence of the proposed method compared with the conventional SBL CE for SNR = 10 dB.

4. Simulation Results

The performance of the proposed F-SBL algorithm was compared with conventional techniques, LS [13], OMP [5], SBL, and TMSBL [7] for a UWA OFDM system with the parameters in Table 1. For the F-SBL algorithm, optimal weights ($w_1^* = 0.4$ and $w_2^* = 0.6$) were employed. In order to investigate the effectiveness of the proposed LR in (21), TMSBL adopted with the proposed LR (F-TMSBL) was also considered. The optimal weights for F-TMSBL were numerically found to be $w_1^* = 0.1$ and $w_2^* = 2.2$. The maximum number of iterations N_{iter} was set to 5 for the F-SBL and F-TMSBL algorithms. For other considered methods, N_{iter} was set to 10, large enough to ensure the best possible performance. The channel having random delay, as described in the Section 3.3, also assessed the performance under diverse underwater conditions.

Figure 4 shows the MSE performance for the time-invariant underwater channel. We can see that the MSE of all considered SBL-based methods decreased for the increasing SNR, while that of OMP exhibited an error floor. The proposed F-SBL outperformed the conventional SBL and performed very close to that of TMSBL. The proposed F-TMSBL had the best MSE performance. TMSBL [7] used multiple OFDM symbols to exploit temporal correlation of the UWA channel, and, subsequently, had a better estimation performance than the original SBL method. It can be confirmed by the superior performance of F-SBL and F-TMSBL algorithms that the proposed LR enhanced the estimation performance.

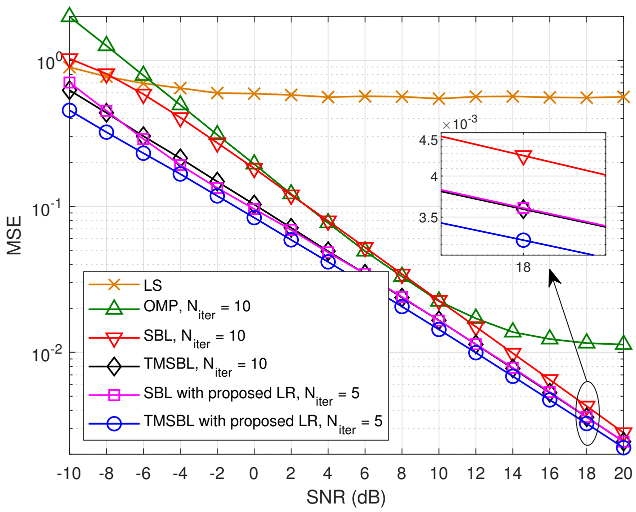

Figure 4. MSE performance versus SNR.

Figure 5 showed the BLER performance for the 16QAM modulation for the time-varying UWA channel. Note that, to induce time-varying characteristics, the Doppler rate of each path was set to $\alpha_l = v_p/c$, $c = 1500$ m/s, where v_p was the relative speed between the transmitter and receiver and had a uniform distribution with a standard velocity deviation of 0.1 m/s. We can observe that the proposed algorithms outperformed the other considered methods. In particular, F-SBL and F-TMSBL algorithms exhibited gains of 0.5 and 0.15 dB at BLER = 0.01 over the original SBL and TMSBL, respectively. Note that this performance gain was obtained even with the number of iterations half of that of other methods. Therefore, the performance analysis confirmed that the proposed method achieved an accurate channel estimation performance with much fewer iterations, which greatly reduced the computational delay and power consumption of the receiver.

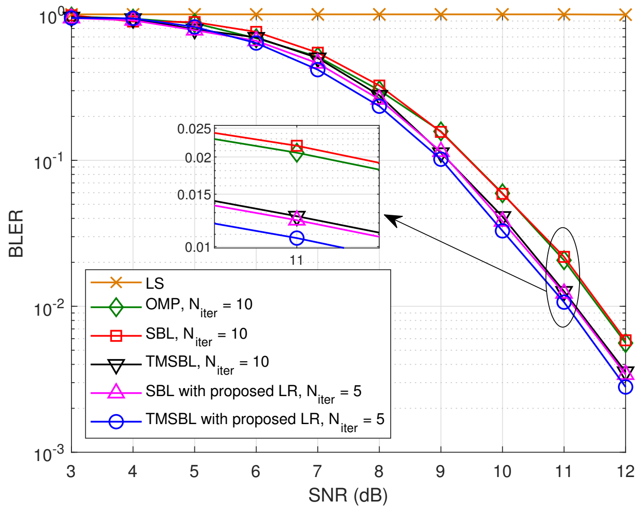

Figure 5. BLER performance versus SNR for 16QAM modulation.

5. Experimental Results

The proposed F-SBL method was applied to experimental UWA OFDM signals to further verify the performance in real underwater conditions. The signals were acquired in an at-sea experiment performed in the Western Sea of Korea from 19 to 20 August 2018. The UWA OFDM system with the parameters in Table 1 was used. A total of 17 frames were transmitted throughout the experimental period. Each frame was composed of 54 OFDM symbols that carried OPSK modulated symbols encoded via a turbo-code (with a code rate of 1/3). The communication range was between 2500 and 3500 m, and the measured sea depth was about 30 m. The underwater CIR estimate corresponding to each frame is shown in Figure 6. We can clearly see that the channel had time-varying characteristics and multi-paths with long delays.

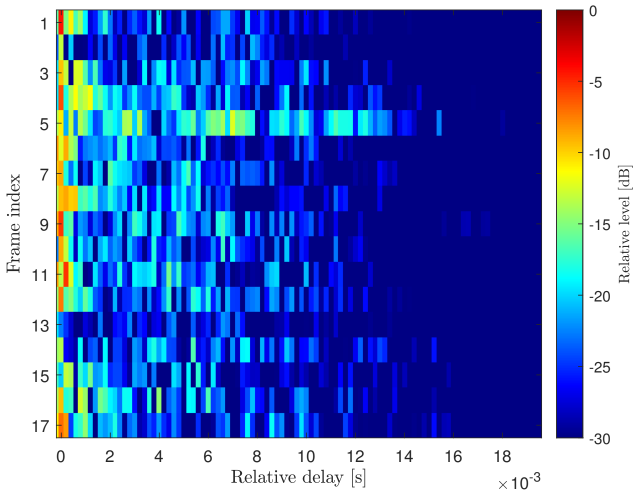

Figure 6. CIR estimate during the whole experimental period.

Figure 7 shows the coded BER performance according to the frame index. It can be observed from the experimental results that the proposed F-SBL and F-TMSBL outperformed the conventional schemes. F-TMSBL yielded the largest error-free reception number, achieving the best BLER. F-SBL exhibited lower-coded BER than the conventional SBL method even with fewer iterations. The experimental results confirm the effectiveness of the proposed method for real underwater channels.

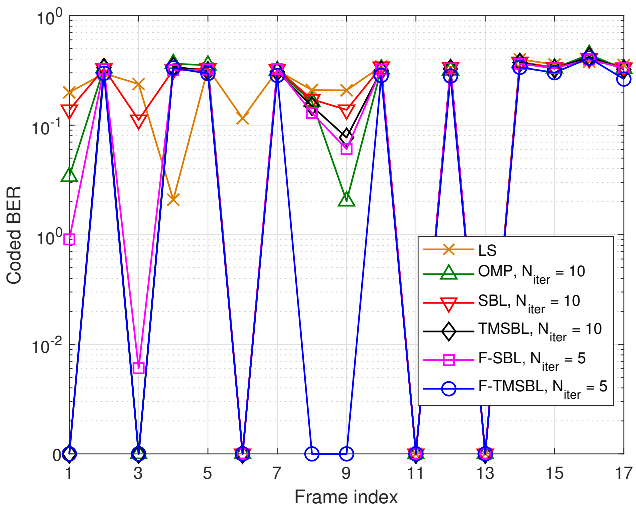

Figure 7. Coded BER performance in at-sea experiment.

6. Conclusions

An F-SBL algorithm based on a weighted LR for hyperparameters is proposed for the channel estimation in a UWA-OFDM system. It was observed that the channel estimate of the SBL algorithm was determined more by the posterior mean rather than the posterior covariance. The proposed weighted LR for hyperparameters was devised to exploit the above observations, enabling not only fast convergence but also more accurate channel estimations. It was confirmed by simulation results that the proposed algorithm achieved higher accuracy in the channel estimation with fewer iteration numbers in comparison to the conventional SBL-based methods for a time-varying UWA channel.

Funding: This research was supported by a grant from the Endowment Project of the “Development of core technologies of underwater robot ICT for polar under-ice-shelf exploration and remote monitoring” funded by Korea Research Institute of Ships and Ocean engineering (PES4390).

Institutional Review Board Statement: Not applicable.

Informed Consent Statement: Not applicable.

Data Availability Statement: Not applicable.

Conflicts of Interest: The author declares no conflict of interest.

Abbreviations

The following abbreviations are used in this manuscript:

USN	underwater sensor network
AUV	autonomous underwater vehicle
UWA	underwater acoustic
OFDM	orthogonal frequency division multiplexing
CE	channel estimator
CS	compressed sensing
SBL	sparse Bayesian learning
TMSBL	temporal multiple SBL
F-SBL	fast SBL
LR	learning rule
AWGN	additive white Gaussian noise

References

1. Karim, S.; Shaikh, F.K.; Chowdhry, B.S.; Mehmood, Z.; Tariq, U.; Naqvi, R.A.; Ahmed, A. GCORP: Geographic and cooperative opportunistic routing protocol for underwater sensor networks. *IEEE Access* **2021**, *9*, 27650–27667. [CrossRef]
2. Wu, J.; Song, C.; Ma, J.; Wu, J.; Han, G. Reinforcement Learning and Particle Swarm Optimization Supporting Real-Time Rescue Assignments for Multiple Autonomous Underwater Vehicles. *IEEE Trans. Intell. Transp. Syst.* **2021**, *23* , 6807–6820. [CrossRef]
3. Stojanovic, M.; Preisig, J. Underwater acoustic communication channels: Propagation models and statistical characterization. *IEEE Commun. Mag.* **2009**, *47*, 84–89. [CrossRef]
4. Huang, J.; Berger, C.R.; Zhou, S.; Huang, J. Comparison of basis pursuit algorithms for sparse channel estimation in underwater acoustic OFDM. In Proceedings of the OCEANS'10 IEEE, Sydney, Australia, 24–27 May 2010; pp. 1–6.
5. Berger, C.; Zhou, S.; Preisig, J.; Willett, P. Sparse Channel Estimation for Multicarrier Underwater Acoustic Communication: From Subspace Methods to Compressed Sensing. *IEEE Trans. Signal Process.* **2010**, *58*, 1708. [CrossRef]
6. Huang, J.; Huang, J.; Berger, C.R.; Zhou, S.; Willett, P. Iterative sparse channel estimation and decoding for underwater MIMO-OFDM. *EURASIP J. Adv. Signal Process.* **2010**, *2010*, 460379. [CrossRef]
7. Qiao, G.; Song, Q.; Ma, L.; Liu, S.; Sun, Z.; Gan, S. Sparse Bayesian learning for channel estimation in time-varying underwater acoustic OFDM communication. *IEEE Access* **2018**, *6*, 56675–56684. [CrossRef]
8. Wang, S.; Li, D.; Liu, M.; Huang, W.; Chen, H.; Cen, Y. Clustered-Sparse Bayesian Learning for Channel Estimation in Underwater Acoustic OFDM Systems. In Proceedings of the 2020 International Conference on Wireless Communications and Signal Processing (WCSP), Nanjing, China, 21–23 October 2020; pp. 546–551.
9. Qin, X.; Qu, F.; Zheng, Y.R. Bayesian iterative channel estimation and turbo equalization for multiple-input–multiple-output underwater acoustic communications. *IEEE J. Ocean. Eng.* **2020**, *46*, 326–337. [CrossRef]
10. Jia, S.; Zou, S.; Zhang, X.; Tian, D.; Da, L. Multi-block Sparse Bayesian learning channel estimation for OFDM underwater acoustic communication based on fractional Fourier transform. *Appl. Acoust.* **2022**, *192*, 108721. [CrossRef]
11. Qiao, G.; Song, Q.; Ma, L.; Sun, Z.; Zhang, J. Channel prediction based temporal multiple sparse bayesian learning for channel estimation in fast time-varying underwater acoustic OFDM communications. *Signal Process.* **2020**, *175*, 107668. [CrossRef]
12. Wang, S.; Liu, M.; Li, D. Bayesian Learning-Based Clustered-Sparse Channel Estimation for Time-Varying Underwater Acoustic OFDM Communication. *Sensors* **2021**, *21*, 4889. [CrossRef] [PubMed]
13. Acar, Y.; Doğan, H.; Panayirci, E. Pilot symbol aided channel estimation for spatial modulation-OFDM systems and its performance analysis with different types of interpolations. *Wirel. Pers. Commun.* **2017**, *94*, 1387–1404. [CrossRef]
14. Xu, T.; Tang, Z.; Leus, G.; Mitra, U. Multi-rate block transmission over wideband multi-scale multi-lag channels. *IEEE Trans. Signal Process.* **2012**, *61*, 964–979. [CrossRef]
15. Zhao, Y.; Yu, H.; Wei, G.; Ji, F.; Chen, F. Parameter estimation of wideband underwater acoustic multipath channels based on fractional Fourier transform. *IEEE Trans. Signal Process.* **2016**, *64*, 5396–5408. [CrossRef]
16. Li, B.; Zhou, S.; Stojanovic, M.; Freitag, L.; Willett, P. Multicarrier communication over underwater acoustic channels with nonuniform Doppler shifts. *IEEE J. Ocean. Eng.* **2008**, *33*, 198–209.
17. Wipf, D.P.; Rao, B.D. Sparse Bayesian learning for basis selection. *IEEE Trans. Signal Process.* **2004**, *52*, 2153–2164. [CrossRef]
18. Tipping, M. The relevance vector machine. In Proceedings of the Advances in Neural Information Processing Systems, Denver, CO, USA, 29 November–4 December 1999; Volume 12.

19. MacKay, D.J. Bayesian interpolation. *Neural Comput.* **1992**, *4*, 415–447. [CrossRef]
20. Kay, S.M. *Fundamentals of Statistical Signal Processing*; Prentice Hall PTR: Hoboken, NJ, USA, 1993.